

# High-density amorphous phase of GeS<sub>2</sub> glass under pressure

Murat Durandurdu

Department of Physics, University of Texas at El Paso, El Paso, Texas 79968, USA

(Received 11 December 2008; revised manuscript received 19 February 2009; published 7 May 2009)

The pressure-induced phase transition in amorphous germanium disulfide (*a*-GeS<sub>2</sub>) is studied using an *ab initio* constant-pressure technique. With the application of hydrostatic pressure, *a*-GeS<sub>2</sub> undergoes a gradual phase transition from a semiconducting low-density amorphous state to a metallic high-density amorphous state. The transition is associated with a local coordination change in both the Ge atoms and S atoms. Upon pressure release, the high-density phase transforms back to a low-density amorphous state. The physical origin of the gradual phase transformation is discussed. The pressure-induced changes in the electronic and vibrational properties are studied with details. Additionally the pressure-induced phase transition of the monoclinic GeS<sub>2</sub> is compared with that of amorphous state.

DOI: 10.1103/PhysRevB.79.205202

PACS number(s): 61.43.Fs, 61.43.Bn

## I. INTRODUCTION

Polyamorphism<sup>1</sup> refers to distinct amorphous states with different densities and bonding environments and is of interest both as a scientific phenomenon and because of its implications in materials processing. For glasses, it is typically induced by external pressure. All of the materials reported to exhibit polyamorphism in their glassy state, such as amorphous ice,<sup>2</sup> silicon<sup>3–6</sup> germanium,<sup>7,8</sup> silica,<sup>9–11</sup> chalcogenide glasses,<sup>12–14</sup> and B<sub>2</sub>O<sub>3</sub> (Refs. 15–19), have tetrahedral coordination environments. At 77 K, ice changes from a low-density amorphous (LDA) phase to a high-density amorphous (HDA) phase under pressure in a first-order transformation.<sup>2</sup> Amorphous Si (Refs. 3–6) and Ge (Refs. 7 and 8) show a sharp transition to a metallic HDA state. Contrary, in other network glasses such as silica,<sup>9–11</sup> germanate,<sup>20</sup> and B<sub>2</sub>O<sub>3</sub> (Refs. 15–19), polyamorphic phase transition can be sluggish because of kinetic reasons and the transition proceeds gradually. Additionally, the HDA phase of these systems cannot be quenched down to ambient pressure but instead transforms back to their original state on decompression. See an excellent review paper for more information about polyamorphic phase transformations.<sup>21</sup>

In contrast to the large body of research done on some glassy systems, the attention on polyamorphic phase transitions in chalcogenide glasses has been insufficient. To date, a few studies have revealed polyamorphic phase transitions in chalcogenide glasses during compression or quenching. Both theoretical<sup>12</sup> and experimental<sup>13,14</sup> studies provide direct evidence for a gradual amorphous-to-amorphous phase transition in glass GeSe<sub>2</sub>. Recent experiment, on the other hand, finds a first-order polyamorphic phase transformation in a Ge<sub>2.5</sub>As<sub>51.25</sub>S<sub>46.25</sub> system.<sup>22</sup> The existence of structurally and thermodynamically distinct phases in amorphous GeS<sub>2</sub> (*a*-GeS<sub>2</sub>) has been demonstrated in several experiments as well. Miyauchi *et al.*<sup>23</sup> showed that *a*-GeS<sub>2</sub> is permanently densified at 573 K and the density of the samples reaches a constant value in the pressure range from 6 to 9 GPa. The densified structures consist of tetrahedral GeS<sub>4</sub> building blocks and the Ge-S bond lengths elongate slightly with increasing density of the samples. In the same study, the formation of a three-dimensional crystalline structure has been also observed around 900 K at 6 GPa. In a Raman-scattering investigation,<sup>24</sup> on the other hand, the sample is found to

remain amorphous with a continuous decrease in Ge-S bond lengths up to 10 GPa at 300 K and the pressure-induced structural and optical changes are found to be reversible upon decompression. Tanaka<sup>25</sup> reported that *a*-GeS<sub>2</sub> is modified from a layerlike structure to a continuous random network and its optical gap decreases gradually with increasing pressure. Temperature is known to have a large influence on this system. Shimada and Dache<sup>26</sup> found that the crystallization of *a*-GeS<sub>2</sub> is kinetically hindered below 573 K and the amorphous network transforms partially into another amorphous state at 3 GPa.

In spite of these experiments, the underlying mechanisms of polyamorphic phase transition in *a*-GeS<sub>2</sub> and detailed information about the structural phase transformation, in particular, the atomic structure of its distinct amorphous states, are still lacking. In this paper, we apply an *ab initio* constant-pressure technique to explore the pressure-induced phase transition in *a*-GeS<sub>2</sub>. Our findings indicate that the amorphous-to-amorphous phase transition proceeds continuously in the model. The transformation is associated with a gradual coordination change in both Ge and S atoms. Such a coordination modification, as expected, leads to a gradual closing of the band-gap energy in a wide pressure range and finally the metallization of the model. The LDA-HDA transition is found to be reversible.

## II. COMPUTATIONAL METHOD

A local-orbital first-principles quantum molecular dynamic (MD) method of Sankey and Niklewski<sup>27</sup> was used in the present study. The method employs the density-functional theory within the local-density approximation and the Harris functional with hard norm-conserving pseudopotentials. The short-range nonorthogonal single- $\zeta$  ( $1s+3p$  per site) local-orbital basis of compact slightly excited *fireball* orbitals of Sankey and Niklewski offered an accurate description of the chemistry with a significant computational advantage. This Hamiltonian with the Parrinello-Rahman<sup>28</sup> method successfully reproduced pressure-induced phase transitions in wide ranges of amorphous and crystalline systems.<sup>3,7,12</sup> Pressure was increased with an increment of 5.0 GPa and at each applied pressure the system was fully relaxed until the maximum force is smaller than 0.02 eV/Å.

The structural minimization was performed with a conjugate-gradient technique. We use  $\Gamma$ -point sampling for the supercell's Brillouin-zone integration.

In order to model *a*-GeS<sub>2</sub> model, the two-dimensional layered GeS<sub>2</sub> crystalline structure was melted at 2000 K about 2 ps. In a period of 2 ps, the temperature was gradually decreased to 1000 K. At this temperature, the system was equilibrated at about 2 ps and then the system was quenched to 0 K. During the quenching, the volume of the simulation cell at zero pressure was optimized using the Parrinello-Rahman pressure-controlling technique. Finally, the structure was relaxed until the maximum force was less than 0.02 eV/Å.

Once the equilibrium configurations under pressure are obtained, we perform the dynamical matrix calculation, displacing every atom in the cells in three orthogonal directions (0.03 Å) and computing the resulting spring constants as second derivatives of the total energy of the system. Diagonalizing the dynamical matrix we receive its eigenvectors and corresponding squared normal-mode frequencies (eigenvalues), which enable us to carry out the full investigation of the vibrational behavior of the equilibrium configurations.

### III. RESULTS

#### A. Pressure-induced phase transition of crystalline GeS<sub>2</sub>

The previous simulations indicate that this *ab initio* technique is very successful in producing realistic amorphous *a*-GeS<sub>2</sub> models<sup>29-31</sup> and in predicting a novel high-pressure phase of GeS.<sup>32</sup> Nevertheless, we further test the technique for the two-dimensional-layered GeS<sub>2</sub> crystalline structure. The structure has monoclinic *P2<sub>1</sub>/c* symmetry and consists of GeS<sub>4</sub> tetrahedra. One half of the tetrahedra in the GeS<sub>2</sub> crystal are edge shared, while the other half are corner shared. The structure was subjected to a hydrostatic pressure and allowed to find its equilibrium state. The pressure-volume relation is illustrated in Fig. 1. At the pressure of 22.0 GPa, the volume shows a discontinuity, which is a characteristic of a first-order phase transition. The structural examination reveals that the two-dimensional-layered structure transforms into a metallic two-dimensional-layered CdI<sub>2</sub>-type structure as shown in Fig. 2. This phase consists of GeS<sub>6</sub> building blocks that are arranged in layers linked by the edges and the corners. This observation clearly suggests that the *ab initio* technique is very successful in reproducing the experimentally determined high-pressure phase of GeS<sub>2</sub> (Ref. 33) and hence it can be used to explore the pressure-induced phase transition in amorphous GeS<sub>2</sub>.

#### B. Pressure-induced phase transition of *a*-GeS<sub>2</sub>

Figure 1 shows the equation of state for the GeS<sub>2</sub> model under pressure. As can be seen from the figure, the volume decreases monotonically, implying that the pressure-induced phase transition in the amorphous model proceeds continuously in stark contrast to the crystalline state. The structural analysis reveals that the LDA phase of GeS<sub>2</sub> gradually transforms into HDA phases (see Fig. 3) and hence the transition between distinct amorphous forms of GeS<sub>2</sub> can be consid-

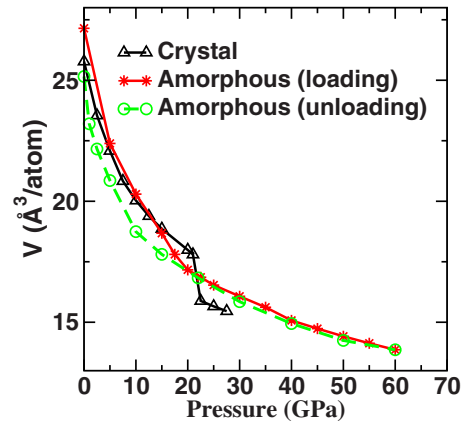


FIG. 1. (Color online) The pressure-volume curve of the crystalline and amorphous GeS<sub>2</sub>. The crystalline GeS<sub>2</sub> transforms from *P2<sub>1</sub>/c* to CdI<sub>2</sub>-type structure at 22 GPa with a discontinuous volume change while its amorphous form gradually transforms into a high-density amorphous phase. Upon pressure release, the high-density amorphous phase transforms back to a low-density amorphous phase.

ered as a relaxation phenomenon as seen in SiO<sub>2</sub>, GeO<sub>2</sub>, and *a*-GeSe<sub>2</sub>.

Upon pressure release from 60 GPa, the path followed is reversed up to 20 GPa at which point the curve develops a hysteresis. Nevertheless, a lower-coordinated amorphous state is recovered with a slightly different density and topology relative to the initial amorphous network. This behavior clearly shows that the LDA-HDA transformation of GeS<sub>2</sub> is reversible.

The average coordination modifications as a function of pressure are depicted in Fig. 4. During the compression, the

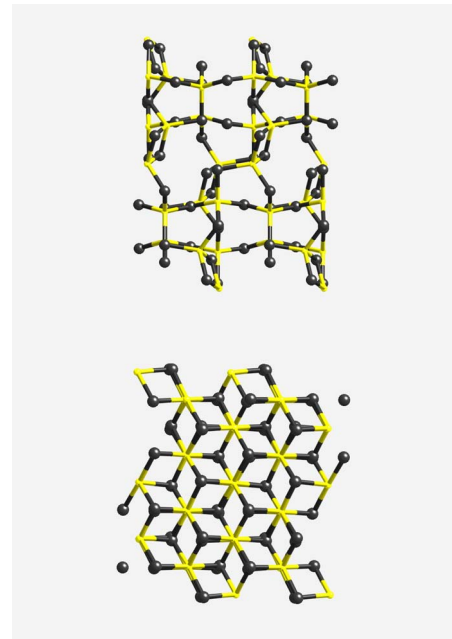


FIG. 2. (Color online) Crystalline GeS<sub>2</sub> within *P2<sub>1</sub>/c* symmetry (top panel) at zero pressure and the two-dimensional layered CdI<sub>2</sub>-type structure (bottom panel) formed at 22 GPa in constant-pressure simulations.

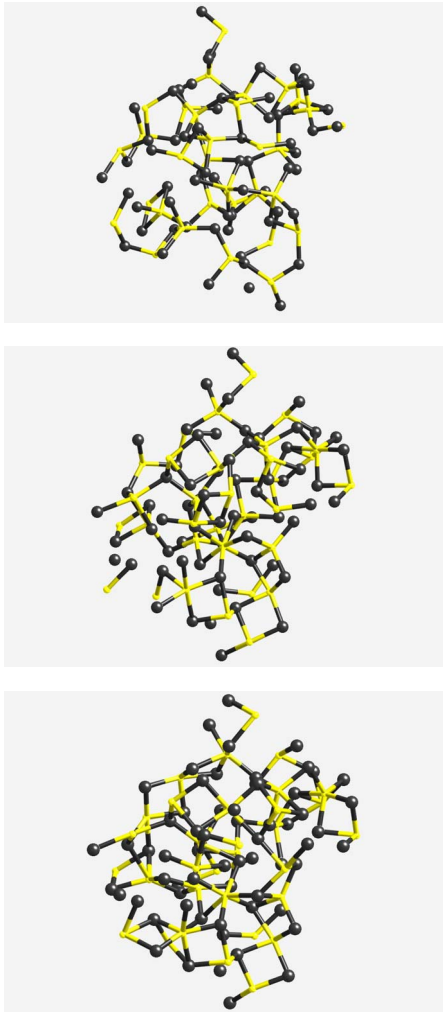


FIG. 3. (Color online) The amorphous model at zero pressure (top panel). The HDA phase at 30 GPa (middle panel) and the HDA phase at 60 GPa (bottom panel).

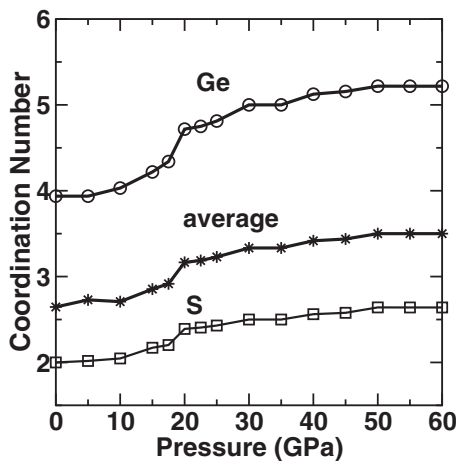


FIG. 4. The coordination changes in the amorphous GeS<sub>2</sub> model as a function of pressure. The coordination of Ge and S atoms gradually increases with increasing pressure and becomes pronounced between 15 and 20 GPa.

LDA state of GeS<sub>2</sub> exhibits a slight modification up to 15.0 GPa. A noticeable coordination change is, however, presented in the model between 15 and 20 GPa. Thereafter, the coordination increase becomes slower again. At 60.0 GPa the average coordination of Ge and S atoms is about 5.21 and 2.64, respectively. At this pressure, only 37.5% of Ge atoms is sixfold coordinated and 46.875% and 15.625% of Ge atoms are fivefold and fourfold coordinated, respectively. The HDA phase at 60 GPa consists of fourfold-(6.25%), threefold-(51.5%), and twofold-(42.25%) coordinated S atoms. A close analysis of the structure indicates that the octahedrally coordinated atoms in the amorphous model are very similar to that formed in CdI<sub>2</sub>-like structure. The coordination change in the model under pressure is summarized in Table I.

In order to shed some light on the amorphous-to-amorphous phase transition in the *a*-GeS<sub>2</sub> model at the atomistic level, we next analyze the structural changes in terms of the real-space partial-pair distribution functions shown in Fig. 5. At zero pressure, the Ge-S distribution has the nearest-neighbor peak around 2.2 Å, which agrees with the experimental value of 2.21 Å (Ref. 34). For the case of the Ge-Ge partial, the peaks at 2.93 Å and 3.59 Å are produced by the edge and corner-sharing tetrahedra, respectively. These values are also close to the experimental distances of 2.91 Å and 3.42 Å (Ref. 34). The peak around 2.2 Å in the S-S correlation is an indication of the existence of S-S wrong bond but the fraction of the wrong bond is very small. The second peak in the S-S pairs is centered at 3.66 Å, which is in perfect agreement with experimental result of 3.64 Å (Ref. 34). With the application of pressure, the intensity Ge-S peak gradually decreases with a broadened distribution and its position slightly shift to larger distance above 15 GPa because of a noticeable increase in the coordination number. In the Ge-Ge partial, the peaks centered at 2.93 and 3.59 Å have a tendency to merge a broad one under pressure. At 15 GPa these peaks merge to a single peak. Above 30 GPa, the formation of Ge-Ge homopolar bonds is observed as indicated by the appearance of a new peak at about 2.4 Å. With increasing pressure the portion of the homopolar bonds increases slightly. For the case of the S-S partial, there is relatively no change seen in the first neighbor S-S lengths while the second-neighbor S-S separations show a dramatic modification and it monotonically decreases toward smaller distances with increasing pressure. Unexpectedly, we do not see any change in the fraction of the S-S homopolar bonds in the network during the pressurizing of the model.

The bond-angle distribution functions shown in Fig. 6 provide additional information regarding the pressure-induced structural changes at the atomistic level. The zero-pressure model exhibits a S-Ge-S distribution with a single peak centered close to the tetrahedral angle. With increasing pressure, the S-Ge-S angles decrease gradually and a new peak around 180° appears in the function. The Ge-S-Ge bond angles have two peaks at 80° and 100°, which are due to edge- and corner-sharing tetrahedra, respectively. As the coordination begins to increase, the peaks smoothly merge to a broad one near 90°. The peaks around 90° and 180° indicate that the high-density amorphous phases partially consist of GeS<sub>6</sub> octahedra.

TABLE I. Coordination number (%) of the amorphous model as a function of pressure. The last column is the zero-pressure model obtained from the pressure release from 60 GPa.

		Pressure (GPa)									
		0	5	10	15	20	30	40	50	60	0
Se	1	10.9	12.5	12.5	10.9	1.56	3.1	1.5			9.3
Se	2	78.1	72.5	70.3	62.5	40.6	50	43.7	42.2	42.2	78.1
Se	3	10.9	15.6	17.2	25	53.1	40.6	51.5	51.5	51.5	12.5
Se	4				1.56	4.68	6.25	3.12	6.25	6.25	
Ge	3	6.25	12.5	3.13	3.12						3.13
Ge	4	93.8	81.3	03.8	81.25	46.9	28.12	15.6	15.63	15.6	93.8
Ge	5		6.25	3.12	6.25	28.1	43.75	56.25	46.87	46.9	3.12
Ge	6				9.37	25	28.12	28.12	37.5	37.5	

We also study the insulator to metal transition in  $a$ -GeS<sub>2</sub>. The calculated density of states as a function of pressure is given in Fig. 7. The zero-pressure model has about 2.3 eV band-gap energy, which is quite less than the experimental result of about 3.2 eV (Ref. 35). We find that the valance-tail states are very sensitive to the pressure and they smoothly shift toward higher energies, causing a closing of the gap. The pronounced decrease in the gap is observed when the increase in coordination begins above 15 GPa. We should underline here that although constant-pressure *ab initio* simulations successfully reproduce high-pressure phases of materials and provide a clear picture about transformation mechanisms, the critical transition pressures predicted in simulations are generally overestimated, in analogy to isobaric superheating in MD simulations. This behavior is indeed associated with the finite size of simulation boxes with periodic boundary conditions as well as the absence of surfaces in simulated structures. Therefore, the coordination

change in  $a$ -GeS<sub>2</sub> and the semiconductor-to-insulator transition pressure are expected to occur in experiments at low-pressure ranges.

We finally investigate the vibrational density of states (VDOS) because the physical origin of the phase transition might be understood by examining the pressure-sensitive soft phonon modes. The computed VDOS at several pressures is given in Fig. 8. The bands shift to higher frequencies with increasing pressure without softening modes; similar to what has been observed in GeSe<sub>2</sub>. At high pressures, the bands overlap because of the significant coordination increase. Particular attention was devoted to vibrational modes with energies around 340 cm<sup>-1</sup>, with regard to the interpretation of features A<sub>1</sub> and A<sub>1</sub><sup>c</sup> modes. A<sub>1</sub> mode at 342 cm<sup>-1</sup> is attributed to symmetric stretch vibrations of S atoms in chains of corner-sharing tetrahedral and A<sub>1</sub><sup>c</sup> mode at 374 cm<sup>-1</sup> is symmetric stretch vibrations of S atoms in bridges of edge-sharing tetrahedra of  $a$ -GeS<sub>2</sub>. No noticeable change is observed in these modes up to 5 GPa. Above this pressure, the

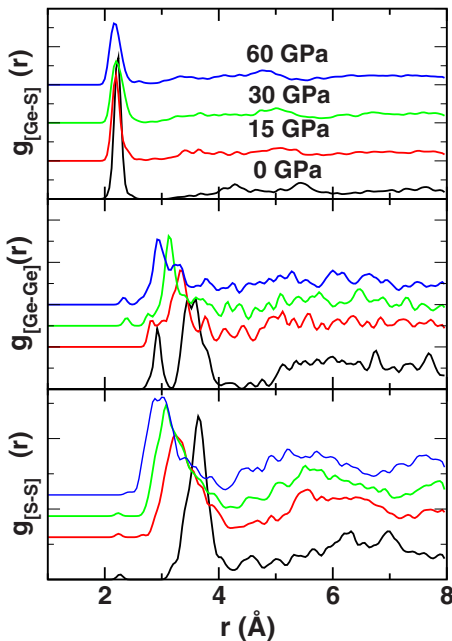


FIG. 5. (Color online) The partial-pair distribution functions at different pressures.

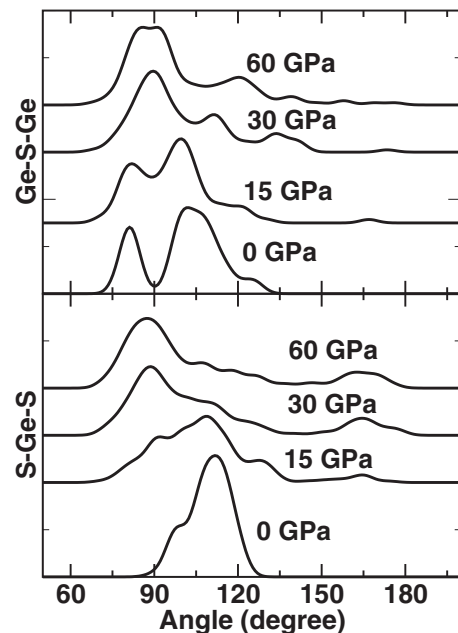


FIG. 6. The bond-angle distribution functions.

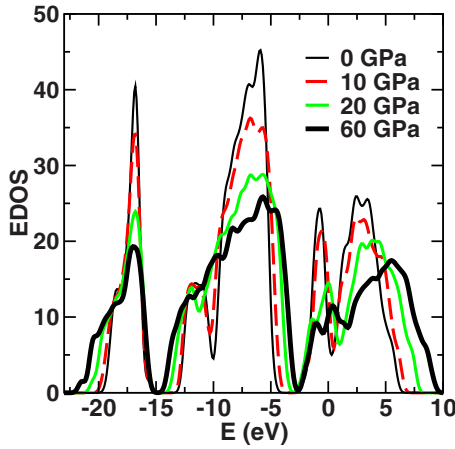


FIG. 7. (Color online) The electron density of states (EDOS) of the amorphous model under pressure. The valence states are more sensitive to the applied pressure and gradually move to the higher energies, causing closing of the band-gap energy.

modes gradually shift to higher frequencies, in agreement with experiment.<sup>24</sup>

### C. Compression of crystalline and amorphous GeS<sub>2</sub> at high pressure

In this section, we will compare the behavior of amorphous and crystalline forms of GeS<sub>2</sub> under pressure. At zero pressure, the volume of amorphous model is slightly larger than the crystalline state. As can be seen from the figure, at low-pressure regimes, the amorphous network presents a more compressible behavior because of its loose structure. Between 5 and 15 GPa both crystalline and amorphous forms have practically identical equation of states. Above this pressure, the amorphous model presents again more compressible behavior.

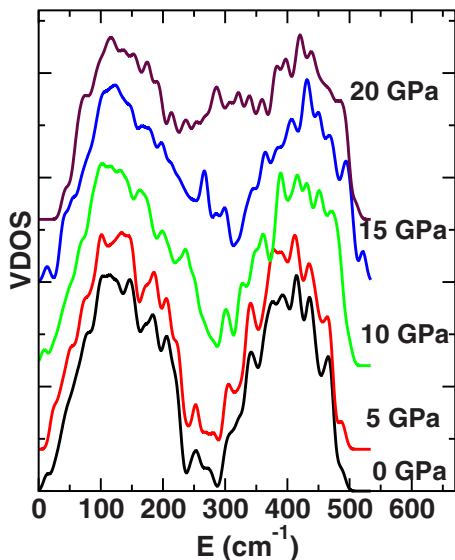


FIG. 8. (Color online) The vibrational density of states of the amorphous model under pressure. The bands shift to higher frequencies with increasing pressure without softening modes.

In contrast to the crystalline state, the coordination number of the HDA phase is not uniform and it consists of differently bounded domains (high and low coordinated). These emphases that the amorphous model partially transforms into a high-density state, having differently coordinated parts (see Table I), in contrast to its crystalline phase. This distinct behavior of the amorphous model can be explained in terms of inhomogeneous stress distributions in the model because of the coordination defects and its disordered nature. Unlike the crystalline structure, the coordination number, bond lengths, and angles of disordered materials are not homogeneous and hence it has a strained topology even at zero pressure. When it is subjected to pressure, the local stress varies from site to site. Therefore, some parts of disordered networks are expected to be more compressible than the other parts. Of course, such a feature in the amorphous model produces nonuniform nucleation and hence a gradual coordination change in some parts of the model. These behaviors differ for the crystalline state in which stress is uniformly distributed on all positions since its coordination number, bonds, and angles have the same values. Therefore in the crystalline state, nucleation occurs homogeneously across the entire lattice structures to conserve the transition symmetry.

The suppression of a first-order phase transition in the amorphous model is another distinct behavior. In the discussion section, we will explain the physical origin of this behavior.

Another important difference between the amorphous and crystalline forms is the coordination number. Although the amorphous model has a much lower density than the crystalline state above 40 GPa, its average coordination number is less than that of the crystalline state.

## IV. DISCUSSION

One of the concerns in *a*-GeS<sub>2</sub> is the quantity of chemical disorder, in particular, the fraction of wrong (homopolar) bonds between like atoms. One can speculate that the existence of the small fraction of homopolar bonds (S-S) and the lack of Ge-Ge homopolar bond in our model at zero pressure is related to the use of a rather small size of the supercell in the simulation, which may artificially favor an amorphous model with almost no chemical disorder. However, recent neutron-diffraction experiment<sup>36</sup> does indeed indicate no evidence for a *significant* number of homopolar bonds in glassy GeS<sub>2</sub> in contrast to Raman spectroscopy.<sup>37</sup> The contradictory result observed in experiments might be associated with sample preparation techniques. Indeed, the atomic structures of amorphous materials are not unique in contrast to crystalline states and they are very sensitive to the experimental procedures. We should note here that the midpoint glass-transition temperature ( $T_g$ ) predicted in these experiments is slightly different. In Ref. 36,  $T_g$  is measured to be 491(5) °C, while  $T_g$  is found to be 502 °C in Ref. 37. Even a small difference in  $T_g$  might result into major differences in the atomic structure of GeS<sub>2</sub>. Additionally, the disorder nature of GeS<sub>2</sub> is very sensitive to sample stoichiometry. A small change in Ge concentration severely alters the resulting amorphous networks. Certainly, further experimental

studies are needed to solve this puzzle. On the other hand, the simulations of a large  $\text{GeS}_2$  model (258 atoms) also imply that the fraction of homopolar bonds is very small<sup>30,31</sup> but it depends on the cooling rate.<sup>31</sup> At a very low cooling rate, 1.9% for the Ge atoms and 1.2% for the S atoms were found to be chemically disordered.<sup>31</sup> These portions are indeed very small, relative to 25% Ge-Ge and Se-Se wrong bonds observed in  $\text{GeSe}_2$ . Definitely, we do have size artifacts in our simulations but their effects on the formation of homopolar bonds appear to be small. Therefore, the zero-pressure model fairly represents the atomic structure of  $\text{GeS}_2$  glass. Moreover, there might exist distinct low-density amorphous forms of  $\text{GeS}_2$  without any chemical disorder. Namely, recent high-pressure experiments have shown that  $\text{GeS}_2$  and the isostructural  $\text{GeSe}_2$  crystal transform into an amorphous state:<sup>38,39</sup> the so-called pressure-induced amorphization. For the case of  $\text{GeSe}_2$ , the amorphous structure induced by pressure appears to be quite different from the amorphous network obtained from the liquid state.<sup>40</sup> Explicitly, Ge-Ge homopolar bonds do not exist in the pressure-induced amorphous form of  $\text{GeSe}_2$  while melt-quenched  $\alpha$ - $\text{GeSe}_2$  has a large fraction of homopolar bonds.

The fraction of chemical disorder appears to be very small. Our model however does not have any Ge-Ge homopolar bonds and hence one might also raise a question here “Can the absence of Ge-Ge wrong bonds in the model affect significantly the atomic structure of resulting HDA phase?” Certainly, it has some influences on the HDA configuration but we do not think that the effect is major because in our previous simulations, we studied the pressure-induced phase transition in two amorphous GaAs networks with different topological properties (The first model is the traditional amorphous Polk-type network and has about 14% of wrong bonds. The second one is the Connell-Temkin type of model with less than 4% of wrong bonds and an almost perfect coordination of four.) and showed that the HDA phase induced by pressure in these two different models had almost the same final configurations (see Ref. 40).

From our simulations, we infer some important results. First one is the modification of the model without showing significant changes in bond lengths and angles below 15.0 GPa, although the volume decreases about 30%. Similar tendency in  $\alpha$ - $\text{GeS}_2$  is also reported in experiments.<sup>25</sup> Of course, such a behavior can be explained by the “free volume” of the amorphous model. Namely, with increasing pressure, the amorphous model transforms into a more closed-packed state by filling its free volume. The second one is the suppression of chemical disorder in the model under pressure up to 30.0 GPa. After this pressure, the model cannot resist to the formation of homopolar bonds, similar to what has been observed in our previous study of  $\text{GeSe}_2$  glass that has a large portion of wrong bonds and amorphous GaAs. The third one is that the pressure-induced phase transition in  $\alpha$ - $\text{GeS}_2$  proceeds gradually in stark contrast to the crystalline  $\text{GeSe}_2$ . A gradual amorphous-to-amorphous phase transformation is commonly seen in binary amorphous compounds, such as GaAs,  $\text{SiO}_2$ ,  $\text{B}_2\text{O}_3$ , and  $\text{GeSe}_2$ , as we mentioned in the introduction section while their crystalline state generally under-

goes a first-order phase transition. In elemental amorphous materials such as Si and Ge, the situation is quite different: their amorphous and crystalline forms show a sharp pressure-induced phase transformation. The different thermodynamic nature of polyamorphic phase transition of elemental and binary amorphous materials is still remaining as an unsolved puzzle in high-pressure community. There might not be a simple explanation of these dissimilar behaviors. Nevertheless, we might speculate the physical origin of the two different behaviors based on present and previous simulations. We find that the pressure significantly suppresses the occurrence of chemical disorder in all binary systems such as GaAs,  $\text{GeSe}_2$ , and  $\text{GeS}_2$  since the formation of wrong bond is not energetically favorable. This might be a key signature for the gradual phase transformation in binary systems. The suppression of chemical disorder makes energetically favorable arrangements in the most stressed parts due to large bond-angle distributions or coordination defects in binary amorphous systems. The local arrangements probably facilitate low-activation pathways for partial coordination changes. Note that the disordered nature of amorphous systems allows the partial coordination changes while this is not the case for crystal in which the transformations occur globally in order to conserve the transition symmetry. Certainly further studies are needed to clearly understand the physical origin of different thermodynamic nature of polyamorphic phase transformations.

## V. CONCLUSIONS

We have studied the pressure-induced phase transition of  $\alpha$ - $\text{GeS}_2$  using constant-pressure *ab initio* technique. The simulation reveals all characteristic of a reversible phase transformation from a low-density amorphous state to a high-density amorphous state in  $\alpha$ - $\text{GeS}_2$ . The transition is gradual and involves in a coordination increase in both Ge and S atoms. As a result of the coordination change, the insulator to metal transition is observed in a wide pressure range. We find that vibration modes shift to higher frequencies with increasing pressure without softening modes and for high-density amorphous phase, the bands overlap. Additionally, we study the pressure-induced phase transformation in crystalline  $\text{GeS}_2$  and find first-order phase transformations into the two-dimensional-layered  $\text{CdI}_2$ -type structure. The amorphous and crystalline forms of  $\text{GeS}_2$  are found to have practically the same equation of state in some pressure ranges. Furthermore, we propose that the gradual amorphous-to-amorphous phase transformation observed in binary amorphous materials is associated with the suppression of chemical disorder during pressurizing of these systems.

## ACKNOWLEDGMENTS

The author is grateful to D. A. Drabold for providing the FIREBALL96 MD code. The calculations were run on Saca-gawea, a 128 processor Beowulf cluster, at the University of Texas at El Paso.

- <sup>1</sup>P. H. Poole, T. Grande, F. Sciortino, H. E. Stanley, and C. A. Angle, *Comput. Mater. Sci.* **4**, 373 (1995).
- <sup>2</sup>O. Mishima, L. D. Calvert, and W. Whalley, *Nature (London)* **314**, 76 (1985).
- <sup>3</sup>M. Durandurdu and D. A. Drabold, *Phys. Rev. B* **64**, 014101 (2001).
- <sup>4</sup>P. F. McMillan, M. Wilson, D. Daisenberger, and D. Machon, *Nature Mater.* **4**, 680 (2005).
- <sup>5</sup>D. Daisenberger, M. Wilson, P. F. McMillan, R. Quesada Cabrera, M. C. Wilding, and D. Machon, *Phys. Rev. B* **75**, 224118 (2007).
- <sup>6</sup>P. F. McMillan, *J. Mater. Chem.* **14**, 1506 (2004).
- <sup>7</sup>M. Durandurdu and D. A. Drabold, *Phys. Rev. B* **66**, 041201(R) (2002).
- <sup>8</sup>A. Di Cicco, A. Congeduti, F. Coppari, J. C. Chervin, F. Baudelet, and A. Polian, *Phys. Rev. B* **78**, 033309 (2008).
- <sup>9</sup>C. Meade, R. J. Hemley, and H. K. Mao, *Phys. Rev. Lett.* **69**, 1387 (1992).
- <sup>10</sup>L. Huang and J. Kieffer, *Phys. Rev. B* **69**, 224203 (2004).
- <sup>11</sup>L. Huang and J. Kieffer, *Phys. Rev. B* **69**, 224204 (2004).
- <sup>12</sup>M. Durandurdu and D. A. Drabold, *Phys. Rev. B* **65**, 104208 (2002).
- <sup>13</sup>Q. Mei, C. J. Benmore, R. T. Hart, E. Bychkov, P. S. Salmon, C. D. Martin, F. M. Michel, S. M. Antao, P. J. Chupas, P. L. Lee, S. D. Shastri, J. B. Parise, K. Leinenweber, S. Amin, and J. L. Yarger, *Phys. Rev. B* **74**, 014203 (2006).
- <sup>14</sup>S. M. Antao, C. J. Benmore, B. Li, L. Wang, E. Bychkov, and J. B. Parise, *Phys. Rev. Lett.* **100**, 115501 (2008).
- <sup>15</sup>L. Huang and J. Kieffer, *Phys. Rev. B* **74**, 224107 (2006).
- <sup>16</sup>S. K. Lee, Kenji Mibe, Yingwei Fei, G. D. Cody, and B. O. Mysen, *Phys. Rev. Lett.* **94**, 165507 (2005).
- <sup>17</sup>S. K. Lee P. J. Eng, Ho-kwang Mao, Y. Meng, M. Newville, M. Y. Hu, and Jinfu Shu, *Nature Mater.* **4**, 851 (2005).
- <sup>18</sup>V. V. Brazhkin, Y. Katayama, K. Trachenko, O. B. Tsiok, A. G. Lyapin, E. Artacho, M. Dove, G. Ferlat, Y. Inamura, and H. Saitoh, *Phys. Rev. Lett.* **101**, 035702 (2008).
- <sup>19</sup>K. Trachenko, V. V. Brazhkin, G. Ferlat, M. T. Dove, and E. Artacho, *Phys. Rev. B* **78**, 172102 (2008).
- <sup>20</sup>O. B. Tsiok, V. V. Brazhkin, A. G. Lyapin, and L. G. Khvostantsev, *Phys. Rev. Lett.* **80**, 999 (1998).
- <sup>21</sup>V. V. Brazhkin and A. G. Lyapin, *J. Phys.: Condens. Matter* **15**, 6059 (2003).
- <sup>22</sup>S. Sen, S. Gaudio, B. G. Aitken, and C. E. Leshner, *Phys. Rev. Lett.* **97**, 025504 (2006).
- <sup>23</sup>K. Miyauchi, J. Qiu, M. Shojiya, Y. Kawamoto, and N. Kitamura, *J. Non-Cryst. Solids* **186**, 279 (2001).
- <sup>24</sup>A. Perakis, I. P. Kotsalas, E. A. Pavlatou, and C. Raptis, *Phys. Status Solidi B* **211**, 421 (1999).
- <sup>25</sup>K. Tanaka, *J. Non-Cryst. Solids* **90**, 363 (1987).
- <sup>26</sup>M. Shimada and F. Dacheille, *Inorg. Chem.* **16**, 2094 (1977).
- <sup>27</sup>O. F. Sankey and D. J. Niklewski, *Phys. Rev. B* **40**, 3979 (1989).
- <sup>28</sup>M. Parrinello and A. Rahman, *Phys. Rev. Lett.* **45**, 1196 (1980).
- <sup>29</sup>S. Blaineau, P. Jund, and D. A. Drabold, *Phys. Rev. B* **67**, 094204 (2003).
- <sup>30</sup>S. Blaineau and P. Jund, *Phys. Rev. B* **69**, 064201 (2004).
- <sup>31</sup>S. Le Roux and P. Jund, *J. Phys.: Condens. Matter* **19**, 196102 (2007).
- <sup>32</sup>M. Durandurdu, *Phys. Rev. B* **72**, 144106 (2005).
- <sup>33</sup>Y. Shimizu and T. Kobayashi, *Mem. Inst. Sci. Technol., Meiji Univ.* **21**, 1 (1983).
- <sup>34</sup>A. Ibanez, M. Bionducci, E. Philippot, L. Descôtes, and R. Bellissent, *J. Non-Cryst. Solids* **202**, 248 (1996).
- <sup>35</sup>K. Tanaka and M. Yamaguchi, *J. Non-Cryst. Solids* **227-230**, 757 (1998).
- <sup>36</sup>I. Petri and P. S. Salmon, *J. Non-Cryst. Solids* **293-295**, 169 (2001).
- <sup>37</sup>L. Cai and P. Boolchand, *Philos. Mag. B* **82**, 1649 (2002).
- <sup>38</sup>Z. V. Popović, Y. S. Raptis, E. Anastassakis, and Z. Jakšić, *J. Non-Cryst. Solids* **227-230**, 794 (1998).
- <sup>39</sup>A. Grzechnik, T. Grande, and S. Stølen, *J. Solid State Chem.* **141**, 248 (1998).
- <sup>40</sup>M. Durandurdu, *Phys. Rev. B* **70**, 085204 (2004).